

## High-pressure structures of lithium, potassium, and rubidium predicted by an *ab initio* evolutionary algorithm

Yanming Ma,<sup>1,2</sup> Artem R. Oganov,<sup>1,3</sup> and Yu Xie<sup>2</sup>

<sup>1</sup>Laboratory of Crystallography, Department of Materials, ETH Zurich, Wolfgang-Pauli-Strasse 10, CH-8093 Zurich, Switzerland

<sup>2</sup>National Laboratory of Superhard Materials, Jilin University, Changchun 130012, People's Republic of China

<sup>3</sup>Geology Department, Moscow State University, 119899 Moscow, Russia

(Received 18 February 2008; revised manuscript received 23 April 2008; published 8 July 2008)

We have extensively explored the high-pressure structures of lithium (Li), potassium (K), and rubidium (Rb) using an *ab initio* evolutionary algorithm. For Li, an unexpected cubic  $P4_132$  structure containing sixfold coordinated lithium atoms and  $\text{Li}_3$  equilateral triangles was discovered to be stable above 300 GPa. This structure is reported for the first time in the elements and shows charge accumulation in the voids of the structure, rather than within the  $\text{Li}_3$  triangles. At pressures above the stability field of complex incommensurate phases, the heavier elements K and Rb were predicted to adopt the sequence of  $I4_1/amd \rightarrow Cmca \rightarrow$  double-hexagonal-close-packed. This sequence parallels the experimentally known structural sequence in Cs, which can be explained by the predominant  $d$  character of the valence electrons in K, Rb, and Cs at high-pressures. The major  $p$  character at the Fermi level in Li makes it distinct from K, Rb, and Cs.

DOI: 10.1103/PhysRevB.78.014102

PACS number(s): 61.66.Bi, 62.50.-p, 64.90.+b

The high-pressure properties of alkali elements are of fundamental interest. These metals are often considered to be “simple” metals as their electronic properties are well described by the nearly free electron model and they adopt the body centered cubic (bcc) form at ambient conditions. The first high-pressure phases for alkali metals are known to have the face-centered cubic (fcc) structure. At still higher pressures, they possess complex crystal structures, unexpected for elemental solids. The post-fcc structural transformations can be understood by the analysis of the transverse acoustic phonon softening and the Fermi surface nesting along the  $\Gamma$ -K symmetry direction in the fcc structure.<sup>1</sup> A pioneer work by Neaton and Ashcroft<sup>2</sup> has proposed a paired “dimer” high-pressure structure ( $\alpha$ -Ga) for Li beyond fcc phase. This is the first research to suggest broken-symmetry structures at high pressure in such a simple metal, and more interestingly, it was further suggested that valence charge buildup occurs only in the interstitials due to the core expulsion under strong compression. The prediction of such intriguing structure extensively stimulated further experimental and theoretical studies to uncover the high-pressure structures of Li. Subsequently, it was experimentally found that fcc Li transforms to the peculiar  $cI16$  phase at 42 GPa through an intermediate rhombohedral modification  $hR1$ .<sup>3</sup> Beyond  $cI16$  structure, the superconductivity<sup>4</sup> and Raman<sup>5</sup> measurements seemed to suggest the existence of a broken-symmetry phase for Li above 60 GPa, but no clear experimental x-ray diffraction data are available to identify its structure. In theory, besides the paired “dimer” ( $\alpha$ -Ga),<sup>2,6</sup> the orthorhombic  $Cmca$ -24 structure<sup>7,8</sup> has been demonstrated to be energetically preferable with respect to the  $cI16$  phase under high pressure.

For heavier alkali metals, K, Rb, and Cs, the post-fcc structural transitions are more complex (see a review in Ref. 9) due to the significant involvement of  $d$  electrons. It is found that fcc K at 23 GPa transforms to an incommensurate host-guest structure (K-III),<sup>10</sup> beyond which no structure determinations have been reported. Nelmes and coworkers<sup>11,12</sup> have demonstrated that fcc Rb transforms into a complex

modulated  $C$ -centered orthorhombic  $C222_1$  structure (Rb-III) at 14 GPa and then into an incommensurate host-guest composite structure (Rb-IV) at 16.6 GPa. On further compression, Rb-IV transforms into the body-centered tetragonal  $I4_1/amd$  structure (Rb-V) at 19.6 GPa<sup>13</sup> and the face-centered orthorhombic  $Cmca$  structure (Rb-VI) at 48.5 GPa,<sup>14</sup> above which no further structures are known. Among the alkali metals, Cs has probably the most complete phase transition sequence reported in the literature: fcc  $\rightarrow$  modulated  $C222_1 \rightarrow I4_1/amd$  (Cs-IV)  $\rightarrow Cmca$  (Cs-V)  $\rightarrow dhcp$  (Cs-VI).<sup>15–19</sup> The intermediate complex structures reflect the fine balance between many competing factors, which include (i) the drive to form denser structures under pressure, (ii) the competition between  $s$  and  $d$  characters of the valence electrons, (iii) repulsion of atomic cores favoring symmetric structures, (iv) exclusionary effect of atomic cores on the valence electrons, leading to lower-symmetry structures and charge density maxima in the voids of the structure, and (v) the Jahn–Teller and Peierls distortions favoring lower-symmetry structures. The formation of the close-packed double hexagonal close packed (dhcp) structure in Cs at 72 GPa may reflect the completion of the  $s \rightarrow d$  electronic transition and/or the dominance of core-core repulsions in the total energy at this and higher pressures. In this respect, dhcp might be viewed as one of the ultimate structures in Cs. Indeed, the dhcp phase was found to be stable at least up to 184 GPa.<sup>18</sup>

Here, we use the *ab initio* evolutionary methodology for crystal structure prediction (see Refs. 20–23 for method descriptions and some of its first applications) to extensively explore the ultrahigh-pressure structures of Li, K, and Rb for a complete understanding of the high-pressure modifications in alkali metals. We focus mainly on the post- $cI16$ , post-K-III, and post-Rb-VI structures for Li, K, and Rb, respectively. Structures of lower-pressure phases of these elements (and all structures of Cs) are well known from experiment, and structures of Na are a very special topic considered in a separate paper.<sup>24</sup>

*Ab initio* evolutionary simulations used here search for the structure possessing the lowest free energy (i.e., the stable structure) at given  $P/T$  conditions and require only the knowledge of the chemical composition. The details of this search algorithm have been described elsewhere.<sup>20–23</sup> The evolutionary search was done with the USPEX code<sup>20–22</sup> and the underlying *ab initio* structure relaxations were performed using density functional theory within the generalized gradient approximation,<sup>25</sup> as implemented in the VASP code.<sup>26</sup> The all-electron projector-augmented wave<sup>27,28</sup> method was adopted. Avoiding core overlap at high pressure, we treat  $1s$  and  $2s$  electrons for Li,  $3s$ ,  $3p$ , and  $4s$  for K, and  $4s$ ,  $4p$ , and  $5s$  for Rb as valence. We used the plane-wave kinetic energy cutoffs of 400 eV for Li, 390 eV for K, and 350 eV for Rb, which were shown to give excellent convergence of the total energies, energy differences, and structural parameters. For computational convenience, we do energy calculations at  $T=0$  K, thus, the free energy reduces to the enthalpy.

We performed variable-cell structure prediction simulations using the above evolutionary methodology at 30, 100, 150, 200, 400, and 1000 GPa with systems containing 4, 6, 8, 12, 16, and 24 atoms in the simulation cell for Li. Among the predicted structures, accurate enthalpy calculations at the particular pressures are performed to derive the most stable structure. Our simulation predicted correctly the fcc and  $cI16$  structures at 30 and 100 GPa, respectively. This gives us confidence to further explore the ultrahigh-pressure phases of Li. At 150 and 200 GPa, our variable-cell simulations predicted that the most stable structure is the Cmca-24, identical to that proposed by Rousseau *et al.*<sup>7</sup> Interestingly, at this pressure regime within the simulation of 4 atom/cell, we also uncovered the paring  $\alpha$ -Ga structure proposed by Neaton and Ashcroft,<sup>2</sup> however, it is metastable with respect to Cmca-24. With pressure increasing up to 400 GPa, the stable structure is found to be the six-coordinated cubic  $P4_132$  with 4 atoms occupying the  $4a$  positions in the unit cell [Fig. 2(c) and Table I]. The lattice parameter  $a$  is 2.391 Å and the nearest Li-Li distance is very short, 1.464 Å (at ambient conditions the Li-Li distance in the bcc phase is 2.026 Å). This cubic structure consists of equilateral triangles ( $Li_3$ ) with three  $Li_3$  units sharing one Li atom as plotted in Fig. 2(c). To the best of our knowledge, this unique structure is reported for the first time in the elements. The only other known elemental phase adopting the rare space group  $P4_132$  is the magnetic  $\beta$ -Mn, but  $\beta$ -Mn has a very different structure with threefold coordination and 20 atoms in the cell.<sup>29</sup> The presence of equilateral  $Li_3$  triangles invites analogy with three-center bonding in boron; however, from the difference charge density plot [Fig. 2(b)], one observes that there is no charge accumulation inside the  $Li_3$  units. The valence electrons are forced away from the regions of significant core overlap into the interstitial space. This can be tracked to the exclusionary effect of atomic cores on valence orbitals, which was pointed out by Neaton and Ashcroft<sup>2</sup> who showed how it can lead to the paring mechanism in the  $\alpha$ -Ga structure; however, in our phase, the  $Li_3$  unit takes over the “ $Li_2$ ” feature. Figure 1 presents the enthalpy curves as a function of pressure for the chosen structures performed at zero temperature. It is clear that the calculation correctly predicts the fcc  $\rightarrow$   $hR1$  and  $hR1 \rightarrow cI16$  transitions at 36.5 and 44 GPa, respectively, in

TABLE I. Lattice parameters and atomic coordinates of the predicted new structures of  $P4_132$  at 400 GPa in Li,  $I4_1/amd$  at 40 GPa, Cmca at 100 GPa, dhcp at 300 GPa in K, and dhcp at 200 GPa in Rb.

Elements	Structures	Lattice constants(Å)	Atomic positions
Li	$P4_132$	$a=2.391$	$4a$ (3/8, 3/8, 3/8)
K	$I4_1/amd$	$a=2.648$ $c=9.916$	$4a$ (0,0,0)
		$a=8.139$	$8f$ (0,0.1751, 0.3271)
	Cmca	$b=4.836$ $c=4.803$	$8d$ (0.2149,0,0)
	dhcp	$a=2.288$ $c=7.525$	$2a$ (0,0,0) $2d$ (1/3,2/3,3/4)
Rb	dhcp	$a=2.582$ $c=8.475$	$2a$ (0,0,0) $2d$ (1/3,2/3,3/4)

excellent agreement with the experimental data of 39 and 42 GPa.<sup>2</sup> The present calculations suggest a stability range of 44–100 GPa for  $cI16$ , above which the Cmca-24 structure has a lower enthalpy. Cmca-24 is found to be stable from 100 to 300 GPa and then the cubic  $P4_132$  takes over. Our phonon calculations at 400 and 600 GPa have verified that the  $P4_132$  structure is dynamically stable by demonstrating the absence of any imaginary phonon frequency in the whole Brillouin zone. Note that we do not include the zero-point (ZP) corrections in the free energy calculations (Fig. 1). However, since Li has very light atomic mass, one might expect a significant ZP contribution. Indeed, the ZP energies for  $\alpha$ -Ga, Cmca-24, and  $P4_132$  structures at 400 GPa are estimated to have large values of 0.1404, 0.1593, and 0.1653 eV/atom, respectively. However, the ZP energy differences between these phases are small, with the maximum values less than 0.025 eV/atom. This fact could not affect the current conclusion. We also have evaluated the temperature effect at 300 K within the quasiharmonic model on the free energy. Again, the resulting energy differences from the temperature contributions between the phases are negligible. It is noteworthy that the structure prediction simulations at 1000 GPa also support the  $Li_3$ -like cubic structure, indicating that the stability field of this phase is at least up to 1000 GPa. Figure 2(a) shows the calculated band structure and electronic density of states (DOS) at 300 GPa. It is obvious that the  $P4_132$  structure is a metal with a relatively low DOS at the Fermi level, in which  $p$  electrons were found to be dominant due to the pressure-induced  $s$ - $p$  charge transfer. With the pressure increased up to 1000 GPa, it is found that Li still remains metallic, thus, we do not support the suggestion of an insulating state under high pressure.<sup>6</sup> However, the shape of the electronic DOS shows that compressed lithium is clearly far from becoming a nearly-free-electron metal even at 1000 GPa. Group analysis suggests two Raman-active phonon modes of  $E$  and  $T_2$  calculated as 939 and 785  $cm^{-1}$ , respectively, at 300 GPa. With pressure increasing up to 800

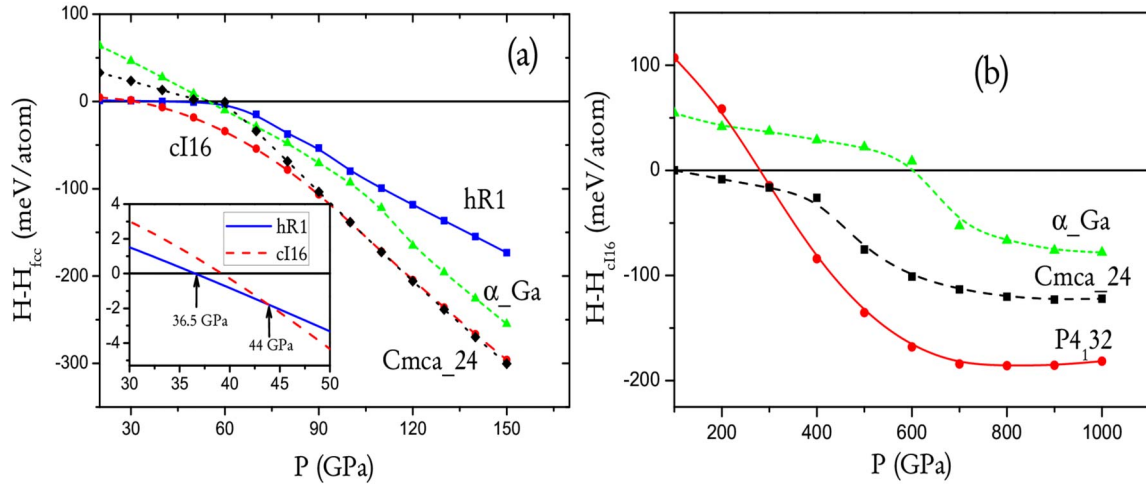


FIG. 1. (Color online) Enthalpy differences (relative to fcc structure) as a function of pressure for  $hR1$ ,  $cI16$ ,  $Cmca$ -24, and  $\alpha$ -Ga structures in Li. The inset clearly shows the  $fcc \rightarrow hR1 \rightarrow cI16$  transition sequence. Bcc structure is not included in this calculation since its stability over fcc is below 7.5 GPa and the pressure scale is thus chosen to start above 20 GPa with fcc structure as the reference to make the figure clearer. (b) Enthalpy differences (relative to the  $cI16$  structure) as a function of pressure for  $P4_32$ ,  $Cmca$ -24, and  $\alpha$ -Ga structures in Li at ultrahigh pressures. We used  $24 \times 24 \times 24$ ,  $24 \times 24 \times 24$ ,  $16 \times 16 \times 16$ ,  $24 \times 24 \times 12$ ,  $16 \times 16 \times 16$ , and  $12 \times 12 \times 12$  Monkhorst-Pack  $k$  meshes for fcc,  $hR1$ ,  $cI16$ ,  $\alpha$ -Ga,  $P4_32$ , and  $Cmca$ -24 structures, respectively. Convergence tests showed that with these settings the total energies were converged to better than 1 meV/atom.

GPa, the Raman modes of  $E$  and  $T_2$  harden to 945 and 842  $\text{cm}^{-1}$ , respectively. However, these Raman frequency values are far below the weak experimental Raman peak at 1800  $\text{cm}^{-1}$  observed at around 120 GPa.<sup>4</sup> Neither our  $P4_32$  structure nor the  $Cmca$ -24 structure and the  $\alpha$ -Ga structure (as shown by Tse *et al.*<sup>8</sup>) can explain such a high-frequency mode. Note that the extremely large phonon frequency of 1800  $\text{cm}^{-1}$  could match a Li-Li distance of 1.24 Å in a linear chain model.<sup>8</sup> As a comparison, the nearest Li-Li distance

in  $P4_32$  structure at 1000 GPa is 1.29 Å, still longer than that (1.24 Å) at 120 GPa. It should be pointed out that a Li-Li distance of 1.24 Å implies a significant core overlap in view of the ionic radius of 0.76 Å in Li. Therefore, at present, there is no explanation for the large discrepancy between theory and experiment in the Raman mode frequencies.

For K, the variable-cell simulations are performed at 40, 100, 150, and 300 GPa with systems containing 4, 6, 8, 12, and 16 in the simulation cell. Our simulation predicted the  $I4_1/amd$  structure at 40 GPa, the  $Cmca$  structure at 100 and 150 GPa, and the  $dhcp$  structure at 300 GPa, respectively. The lattice parameters and atomic coordinates for the three structures are listed in Table I. Note that these three structures are isostructural with Cs-IV, Cs-V, and Cs-VI, respectively. The calculated enthalpy curves for the predicted structures with respect to fcc phase are shown in Fig. 3(a). It is found that the structural sequence beyond K-III in K is  $I4_1/amd \rightarrow Cmca \rightarrow dhcp$ , where the transitions occur at 80 and 250 GPa, respectively. Note that the incommensurate nature of K-III structure precludes us from its enthalpy calculation within the current implementation of the periodic methodology.

The variable-cell simulations for Rb were performed at 40, 70, 100, 150, and 200 GPa with systems containing 4, 6, 8, and 12 atoms in the simulation cell. We correctly uncovered the  $I4_1/amd$  structure at 40 GPa and  $Cmca$  structure at 100 GPa, in excellent agreement with experiment.<sup>13,14</sup> At 150 and 200 GPa, we predicted the  $dhcp$  structure to be the most stable. The calculated enthalpy curves for the three structures (relative to fcc phase) are shown in Fig. 3(b). It can be clearly seen that beyond the Rb-IV phase, the structural sequence is also  $I4_1/amd \rightarrow Cmca \rightarrow dhcp$ , where the transitions occur at 41 and 143 GPa, respectively. Note that the calculated  $I4_1/amd \rightarrow Cmca$  transition pressure is in good

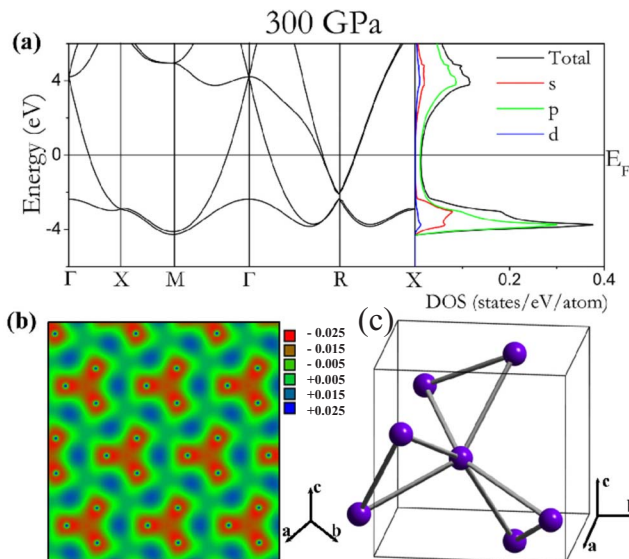


FIG. 2. (Color online) (a) The calculated band structure (left panel) and total and partial electronic DOS (right panel), (b) the difference charge density plot in the plane containing the  $Li_3$  unit, and (c) the schematic of the crystal structure of the predicted cubic  $P4_32$  structure at 300 GPa.



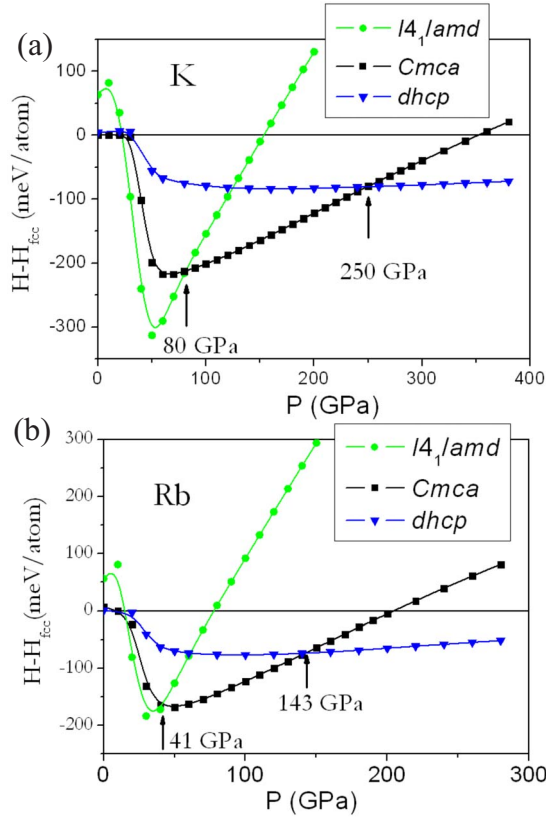


FIG. 3. (Color online) Enthalpy differences (relative to the fcc structure) as a function of pressure for  $I4_1/amd$ ,  $Cmca$ , and  $dhcp$  structures in (a) K and (b) Rb. We used  $12 \times 12 \times 8$ ,  $8 \times 8 \times 8$ , and  $12 \times 12 \times 12$  Monkhorst–Pack  $k$  meshes for  $I4_1/amd$ ,  $Cmca$ , and  $dhcp$  structures, respectively. Convergence tests showed that with these settings the total energies were converged to better than 1 meV/atom.

agreement with the experimental value of 48.5 GPa.<sup>14</sup>

With the current findings, it is suggested that although K, Rb, and Cs have different intermediate complex structures, beyond which, they adopt the same structural transition sequence at higher pressure. Eventually, the three heavier elements are predicted to adopt the same close-packed  $dhcp$  structure. However, a totally different  $P4_132$  structure is predicted to occur in Li at ultrahigh pressures. To understand the origin for the discrepancy, we plot the partial electronic DOS for K, Rb, and Cs in  $dhcp$  structure in Fig. 4. It is found that all these metals are dominated by the  $d$  electrons originated from the  $s$ - $d$  charge transfer under pressure. As a result, the major  $p$  electrons in Li [Fig. 2(a)] make it vastly different from the heavier alkali metals. The situation of Na is also very special; in Na, the orbital character at very high pressures is a  $p$ - $d$  hybrid.<sup>24</sup> As a result, very unusual structural sequences with exotic electronic structure appear at ultrahigh pressures. It is noteworthy that for the heavier elements of K, Rb, and Cs, the  $I4_1/amd$  structure is stabilized only in a narrow pressure range relative to those of  $Cmca$  and  $dhcp$ . This fact might have originated from its intermediate  $d$  popu-

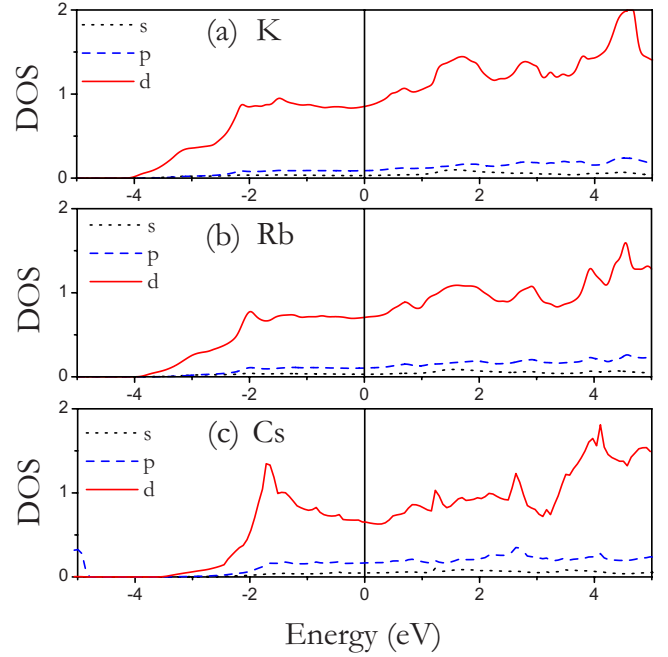


FIG. 4. (Color online) Partial  $s$ ,  $p$ , and  $d$  electronic densities of states for  $dhcp$  K, Rb, and Cs at 380, 300, and 200 GPa, respectively. The Fermi level was set to zero.

lation and low packing density. Upper and lower limits to its stability could thus apply: At low pressures, close-packed structures (fcc) are stable and at high pressures, close packing ( $dhcp$ ) returns, squeezing the stability field of  $I4_1/amd$  in a relatively narrow intermediate pressure range.

In summary, we have extensively explored the ultrahigh-pressure structures of Li, K, and Rb using *ab initio* evolutionary algorithm. We report for the first time a sixfold coordinated cubic  $P4_132$  structure in Li consisting of  $Li_3$  equilateral triangles. This structure shows charge accumulation in the empty space rather than inside the  $Li_3$  triangles. Beyond the intermediate complex (modulated) structures K-III and Rb-IV, the high-pressure structural sequences in heavier elements K and Rb were predicted to adopt  $I4_1/amd \rightarrow Cmca \rightarrow dhcp$ , isostructural with that in Cs, originated from the common  $d$  electrons dominance in these metals. The primary  $p$  characters in Li make it different from K, Rb, and Cs, as well as from Na, where a mixed  $p$ - $d$  character prevails at ultrahigh pressures and leads to unusual physical states. The success in correctly reproducing the fcc and  $cI16$  structures in Li and the  $I4_1/amd$  and  $Cmca$  structures in Rb without any empirical information incorporated in the simulation has not only demonstrated, again, the power of the recently developed evolutionary algorithm in addition to the other successes,<sup>20–23</sup> but also validated our further predictions in Li, K, and Rb.

We thank the Swiss National Science Foundation (Grant No. 200021-111847/1), CSCS, and ETH Zurich for supercomputers.

- <sup>1</sup>Y. Xie, J. S. Tse, T. Cui, A. R. Oganov, Z. He, Y. Ma, and G. Zou, *Phys. Rev. B* **75**, 064102 (2007).
- <sup>2</sup>J. B. Neaton and N. W. Ashcroft, *Nature (London)* **400**, 141 (1999).
- <sup>3</sup>M. Hanfland, K. Syassen, N. E. Christensen, and D. L. Novikov, *Nature (London)* **408**, 174 (2000).
- <sup>4</sup>V. V. Struzhkin, M. I. Erements, W. Gan, H. K. Mao, and R. J. Hemley, *Science* **298**, 1213 (2002).
- <sup>5</sup>A. F. Goncharov, V. V. Struzhkin, H. K. Mao, and R. J. Hemley, *Phys. Rev. B* **71**, 184114 (2005).
- <sup>6</sup>N. E. Christensen and D. L. Novikov, *Solid State Commun.* **119**, 477 (2001).
- <sup>7</sup>R. Rousseau, K. Uehara, D. D. Klug, and J. S. Tse, *ChemPhysChem* **6**, 1703 (2005).
- <sup>8</sup>J. S. Tse, D. D. Klug, and T. Iitaka, *Phys. Rev. B* **73**, 212301 (2006).
- <sup>9</sup>M. I. McMahon and R. J. Nelmes, *Chem. Soc. Rev.* **35**, 943 (2006).
- <sup>10</sup>M. I. McMahon, R. J. Nelmes, U. Schwarz, and K. Syassen, *Phys. Rev. B* **74**, 140102(R) (2006).
- <sup>11</sup>R. J. Nelmes, M. I. McMahon, J. S. Loveday, and S. Rekhii, *Phys. Rev. Lett.* **88**, 155503 (2002).
- <sup>12</sup>M. I. McMahon, S. Rekhii, and R. J. Nelmes, *Phys. Rev. Lett.* **87**, 055501 (2001).
- <sup>13</sup>H. Olijnyk and W. B. Holzapfel, *Phys. Lett. A* **99**, 381 (1983).
- <sup>14</sup>U. Schwarz, K. Syassen, A. Grzechnik, and M. Hanfland, *Solid State Commun.* **112**, 319 (1999).
- <sup>15</sup>M. I. McMahon, R. J. Nelmes, and S. Rekhii, *Phys. Rev. Lett.* **87**, 255502 (2001).
- <sup>16</sup>K. Takemura, S. Minomura, and O. Shimomura, *Phys. Rev. Lett.* **49**, 1772 (1982).
- <sup>17</sup>U. Schwarz, K. Takemura, M. Hanfland, and K. Syassen, *Phys. Rev. Lett.* **81**, 2711 (1998).
- <sup>18</sup>K. Takemura, N. E. Christensen, D. L. Novikov, K. Syassen, U. Schwarz, and M. Hanfland, *Phys. Rev. B* **61**, 14399 (2000).
- <sup>19</sup>K. Takemura, O. Shimomura, and H. Fujihisa, *Phys. Rev. Lett.* **66**, 2014 (1991).
- <sup>20</sup>A. R. Oganov, C. W. Glass, and S. Ono, *Earth Planet. Sci. Lett.* **241**, 95 (2006).
- <sup>21</sup>A. R. Oganov and C. W. Glass, *J. Chem. Phys.* **124**, 244704 (2006).
- <sup>22</sup>C. W. Glass, A. R. Oganov, and N. Hansen, *Comput. Phys. Commun.* **175**, 713 (2006).
- <sup>23</sup>Y. M. Ma, A. R. Oganov, and C. W. Glass, *Phys. Rev. B* **76**, 064101 (2007).
- <sup>24</sup>Y. M. Ma, A. R. Oganov, and Y. Xie (unpublished).
- <sup>25</sup>J. P. Perdew, K. Burke, and M. Ernzerhof, *Phys. Rev. Lett.* **77**, 3865 (1996).
- <sup>26</sup>G. Kresse and J. Furthmuller, *Phys. Rev. B* **54**, 11169 (1996).
- <sup>27</sup>G. Kresse and D. Joubert, *Phys. Rev. B* **59**, 1758 (1999).
- <sup>28</sup>P. E. Blochl, *Phys. Rev. B* **50**, 17953 (1994).
- <sup>29</sup>J. Donohue, *The Structures of the Elements* (Wiley, New York, 1974).